INTERNATIONAL JOURNAL OF MEDICAL SCIENCE AND DENTAL HEALTH
(ISSN: 2454-4191)
www.ijmsdh.org (2026)

Check for updates

Received: 10 Aug 2026
Revised: 25 Aug 2026
Accepted: 11 Sep 2026
Published: 18 Sep 2026

Volume 12 Issue 09, 2026
Page No - 164-175
DOI - 10.55640/ijmsdh-12-09-19

Article Citation: Fayziyeva Nozima Gulom kizi, & Temirova Nazokat Rustamovna. (2026). Age-Dependent Changes in Ki-67 And Bcl-6 Immunohistochemical Expression in Rat Lymph Nodes Under Combined Inhalational Exposure to Pm2.5 And Tobacco Smoke and Their Biocorrection. International Journal of Medical Science and Dental Health, 12(09), 164-175. https://doi.org/10.55640/ijmsdh-12-09-19

Copyright: © 2026 The Authors. Published by IJMSDH under the Creative Commons CC BY License

Age-Dependent Changes in Ki-67 And Bcl-6 Immunohistochemical Expression in Rat Lymph Nodes Under Combined Inhalational Exposure to Pm2.5 And Tobacco Smoke and Their Biocorrection

Fayziyeva Nozima Gulom kizi

Independent Researcher, Bukhara State Medical Institute named after Abu Ali ibn Sina, Uzbekistan

Temirova Nazokat Rustamovna

Associate Professor, Department of Anatomy and Clinical Anatomy, Bukhara State Medical Institute named after Abu Ali ibn Sina, Bukhara, Uzbekistan

Abstract

Background. Ambient fine particulate matter (PM2.5) and tobacco smoke are two of the leading global risk factors, and their combined inhalation damages the adaptive immune system; however, the age-dependent germinal-centre response of regional lymph nodes to such combined exposure, and its correction, are poorly characterized.

Aim. To quantify the proliferative (Ki-67) and germinal-centre B-cell (BCL-6) immunohistochemical profile of tracheobronchial and mediastinal lymph nodes in rats of three ages (6, 12 and 18 months) under combined PM2.5 + tobacco-smoke exposure and after biocorrection with an infusion of Althaea officinalis L. Methods. Ki-67 and BCL-6 were assessed by HRP–DAB immunohistochemistry with digital quantification in QuPath v0.6.0 and semiquantitative IRS (Remmele–Stegner) scoring in control, combined-exposure and biocorrection groups. The recovery rate was defined as (biocorrection − exposure)/(control − exposure) × 100%.

Results. In control animals both markers declined physiologically with age (Ki-67 68→61→54%; BCL-6 24→18→12%). Combined exposure reduced Ki-67 by 47.1%, 52.5% and 59.3% and BCL-6 by 54.2%, 55.6% and 58.3%

relative to age-matched control, deepening with age. Biocorrection restored Ki-67 to 59/51/43% and BCL-6 to 20/15/10%, with recovery rates of 71.9/68.8/65.6% (Ki-67) and 69.2/70.0/71.4% (BCL-6). The immunohistochemical changes paralleled the morphometric germinal-centre reduction. Conclusion. Combined PM2.5 + tobacco-smoke exposure produces a cumulative, age-aggravated "Ki-67↓ + BCL-6↓" suppression of germinal-centre proliferative and B-cell function, and Althaea officinalis exerts a marked but incomplete, protective and functionally restorative (immunomodulatory) effect rather than absolute regeneration.

Keywords: Lymph node, germinal centre, Ki-67, BCL-6, immunohistochemistry, IRS, PM2.5, tobacco smoke, biocorrection, Althaea officinalis, digital pathology, QuPath, rats.

Introduction

Air pollution and tobacco use remain two of the leading preventable global risk factors. In 2021 air pollution was the second-ranked mortality risk factor worldwide (about 8.1 million deaths), with more than 90% attributable to fine particulate matter (PM2.5), while tobacco causes over 8 million deaths annually [1; 2; 3]. Because tobacco smoke is itself a major indoor source of PM2.5, the respiratory tract is frequently exposed to both agents at once [4]. A landmark study demonstrated that inhaled particulates accumulate in human lung-associated lymph nodes over decades, compromising immune surveillance through direct effects on immune-cell function and lymphoid architecture [5; 6]. Experimental and clinical work has further shown that PM2.5 impairs both innate and adaptive immunity, reducing the capacity of immune cells to respond to microbial and antigenic challenge [7; 8], while chronic tobacco-smoke and nicotine exposure suppresses T-cell function in lung-associated lymph nodes and attenuates antigen-specific germinal-centre and antibody responses [9; 10; 11].

The germinal centre is the principal microanatomical site of B-cell proliferation, somatic hypermutation, affinity maturation and memory-cell formation, and is therefore highly sensitive to oxidative and inflammatory injury. Two nuclear markers characterize its functional state: Ki-67, expressed in all active phases of the cell cycle (G_1, S, G_2, M) and an established indicator of proliferative activity [12; 13], and BCL-6, a transcriptional repressor expressed by germinal-centre B cells that governs the germinal-centre reaction [14; 15]. Despite extensive data on PM2.5 and tobacco smoke individually, the age-dependent germinal-centre Ki-67/BCL-6 response to their combined inhalation, and the possibility of pharmacological biocorrection, have not been systematically quantified. The problem addressed here is therefore twofold: to establish how combined exposure reshapes the proliferative and B-cell functional axis of the lymph node across ages, and to determine to what extent an infusion of Althaea officinalis L. — a plant with documented antioxidant, anti-inflammatory and immunomodulatory activity [16; 17] — can restore it. This study provides that quantitative, digitally analysed, IRS-scored immunohistochemical evaluation.

Methods

The study was performed on outbred white rats of three age cohorts (6, 12 and 18 months). At each age three groups were compared: an intact control; a group receiving combined inhalational exposure to PM2.5 (aerosolized ERM®-CZ110 reference dust) and tobacco smoke in a sealed free-breathing chamber; and a biocorrection group receiving, after exposure, an oral infusion of Althaea officinalis L. (100 mg/kg). Tracheobronchial and mediastinal lymph nodes were fixed in 10% neutral buffered formalin and embedded in paraffin. Sections 3–4 μm thick were mounted on adhesive slides, dewaxed and rehydrated; heat-induced antigen retrieval was performed at 98 °C for 30–40 min and endogenous peroxidase was blocked with hydrogen peroxide. Sections were incubated with primary antibodies to Ki-67 and BCL-6 according to the manufacturer's instructions; the reaction was visualized with an HRP-polymer system and DAB chromogen, and nuclei were counterstained with haematoxylin. A distinct brown nuclear signal was scored as positive.

Digital quantification was carried out in QuPath v0.6.0 on ×400 images of germinal centres within a standardized region of interest: total detected nuclei, positive and negative nuclei and the percentage of positive cells were computed automatically. Reactions were graded semiquantitatively by the Immunoreactive Score (IRS) of Remmele and Stegner (1987) as the product of the proportion score (A: 0 = 0%, 1 = 1–10%, 2 = 11–50%, 3 = 51–80%, 4 = > 80%) and the intensity score (B: 0–3), giving IRS = A × B (range 0–12) [18]. To express the effect of biocorrection independently of the physiological age gradient, the recovery rate was calculated as (biocorrection − exposure)/(control − exposure) × 100%. Because the study compared three groups across three ages, group differences at each age and age trends within each group were evaluated; percentage and IRS data — being bounded proportions and ordinal scores — are reported descriptively with the corresponding QuPath cell counts, and the consistency between digital quantification and semiquantitative scoring was used as internal verification [12; 13].

Table 1. Semiquantitative IRS scoring system (Remmele & Stegner, 1987) used for Ki-67 and BCL-6

Proportion of positive cells	Score (A)	Staining intensity	Score (B)
0%	0	No staining	0
1–10%	1	Weak	1
11–50%	2	Moderate	2
51–80%	3	Strong	3
> 80%	4	—	—

Final score: IRS = A × B (range 0–12).

Results

1. Normal age-related Ki-67 and BCL-6 profile (control group)

In control animals of all ages, Ki-67 immunoreactivity was localized mainly to the germinal centres of secondary follicles, in proliferating lymphoblasts and large lymphoid cells, with little expression in the mantle, paracortical zone and medullary cords; the reaction was nuclear, with a sharply demarcated brown DAB signal. BCL-6 was expressed almost exclusively in the nuclei of germinal-centre B cells, with a characteristic topographic (zonal) distribution. Both markers declined progressively with age. Ki-67-positive cells fell from 68% (6 months; IRS 9) to 61% (12 months; IRS 9) and 54% (18 months; IRS 6), and BCL-6-positive cells from 24% (IRS 6) to 18% (IRS 4) and 12% (IRS 4). This physiological "68→61→54%" and "24→18→12%" gradient reflects an age-related decline of germinal-centre proliferative and B-cell functional activity while the zonal organization of the node is preserved (Table 2, Diagram 5).

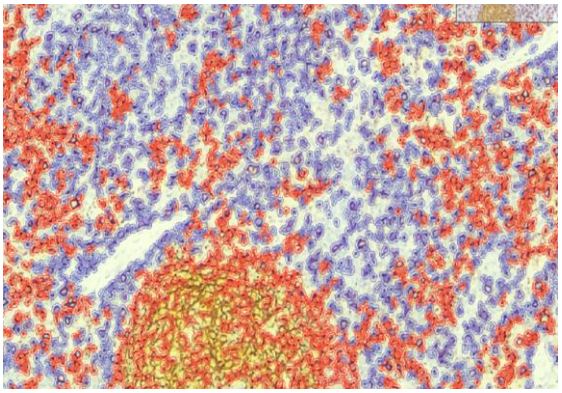

Figure 1. Micrograph placement — Ki-67, control group, 6-month rat. Germinal centre, ×400, DAB. QuPath v0.6.0: 749 detected cells, 509 positive, 68% expression

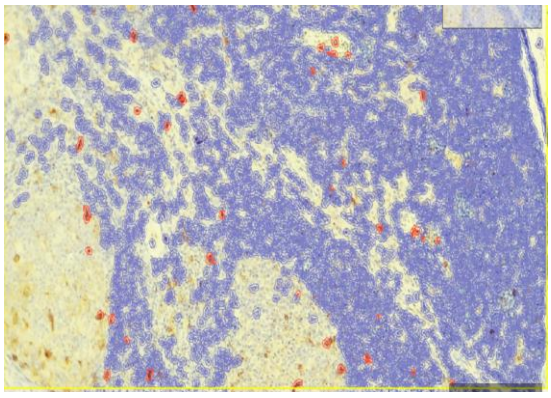

Figure 2. Micrograph placement — BCL-6, control group, 6-month rat. Germinal centre, ×400, DAB. 24% positive expression.

Table 2. Age-related Ki-67 and BCL-6 immunohistochemical expression in the control group

Age	Marker	Positive cells, %	Proportion score (A)	Intensity score (B)	IRS
6 mo	Ki-67	68	3	3	9
	BCL-6	24	2	3	6
12 mo	Ki-67	61	3	3	9
	BCL-6	18	2	2	4
18 mo	Ki-67	54	3	2	6
	BCL-6	12	2	2	4

2. Combined PM2.5 + tobacco-smoke exposure

Combined exposure markedly suppressed both markers at every age, and the suppression deepened with age. Relative to age-matched control, Ki-67-positive cells decreased from 68% to 36% at 6 months (−47.1%; IRS 9→4), from 61% to 29% at 12 months (−52.5%; IRS 9→4) and from 54% to 22% at 18 months (−59.3%; IRS 6→2). Morphologically, Ki-67-positive nuclei became sparse and unevenly, focally distributed within the germinal centres, indicating restriction of the proliferative compartment. These immunohistochemical findings ran in parallel with the morphometric germinal-centre reduction reported previously (e.g. at 18 months the germinal- centre area fell by ≈ 67.2% and its cell number by ≈ 61.2%), confirming a co-directional structural–functional decline.

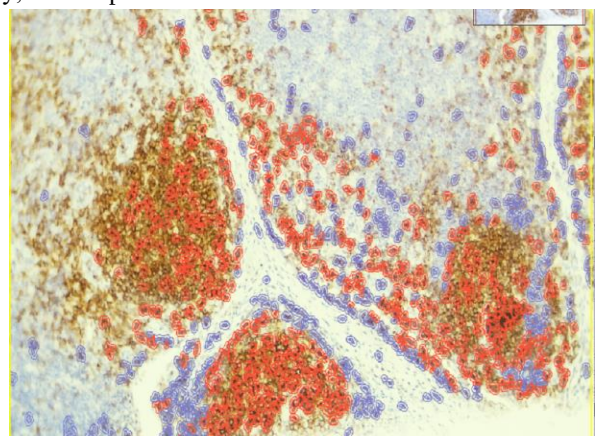

Figure 3. Micrograph placement — Ki-67, combined-exposure group, 6-month rat. ×400, DAB. QuPath: 675 detected, 243 positive, 36% expression.

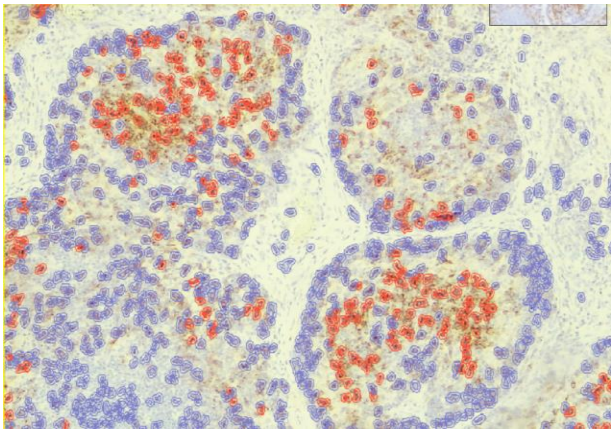

Figure 4. Micrograph placement — Ki-67, combined-exposure group, 18-month rat. ×400, DAB. 22% expression — the lowest across groups.

BCL-6 showed the same pattern. Positive cells fell from 24% to 11% at 6 months (−54.2%; IRS 6→2), from 18% to 8% at 12 months (−55.6%; IRS 4→1) and from 12% to 5% at 18 months (−58.3%; IRS 4→1). At 12 and 18 months the proportion crossed below the 10% threshold, lowering the IRS proportion score from 2 to 1. The residual BCL-6-positive cells retained their germinal-centre topography, indicating a quantitative contraction of the BCL-6-reactive B-cell population rather than a loss of zonal identity (Table 3, Diagrams 1, 2, 7).

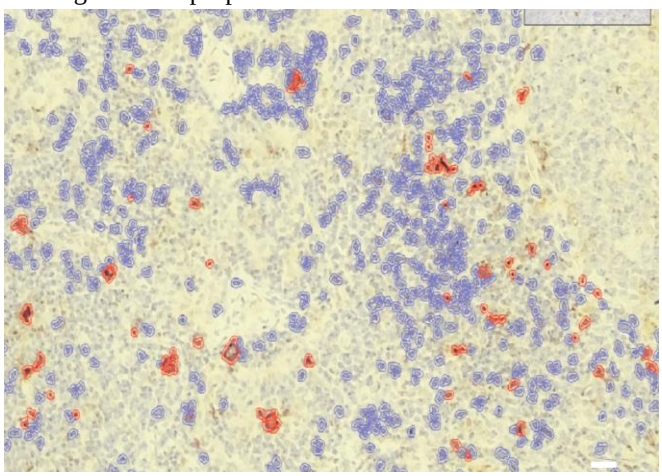

Figure 5. Micrograph placement — BCL-6, combined-exposure group, 6-month rat. ×400, DAB. QuPath: 700 detected, 77 positive, 11% expression.

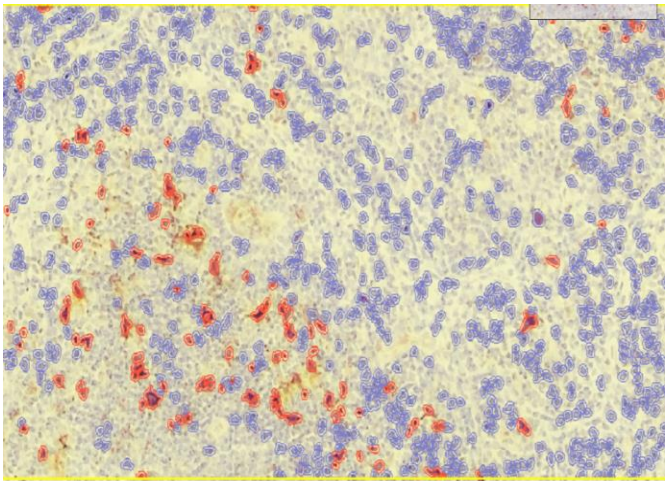

Figure 6. Micrograph placement — BCL-6, combined-exposure group, 18-month rat. ×400, DAB. 5% expression.

Table 3. Ki-67 and BCL-6 expression under combined exposure versus control

Age	Marker	Control, %	Exposure, %	Reduction, %	IRS (C→E)
6 mo	Ki-67	68	36	47.1	9 → 4
	BCL-6	24	11	54.2	6 → 2
12 mo	Ki-67	61	29	52.5	9 → 4
	BCL-6	18	8	55.6	4 → 1
18 mo	Ki-67	54	22	59.3	6 → 2
	BCL-6	12	5	58.3	4 → 1

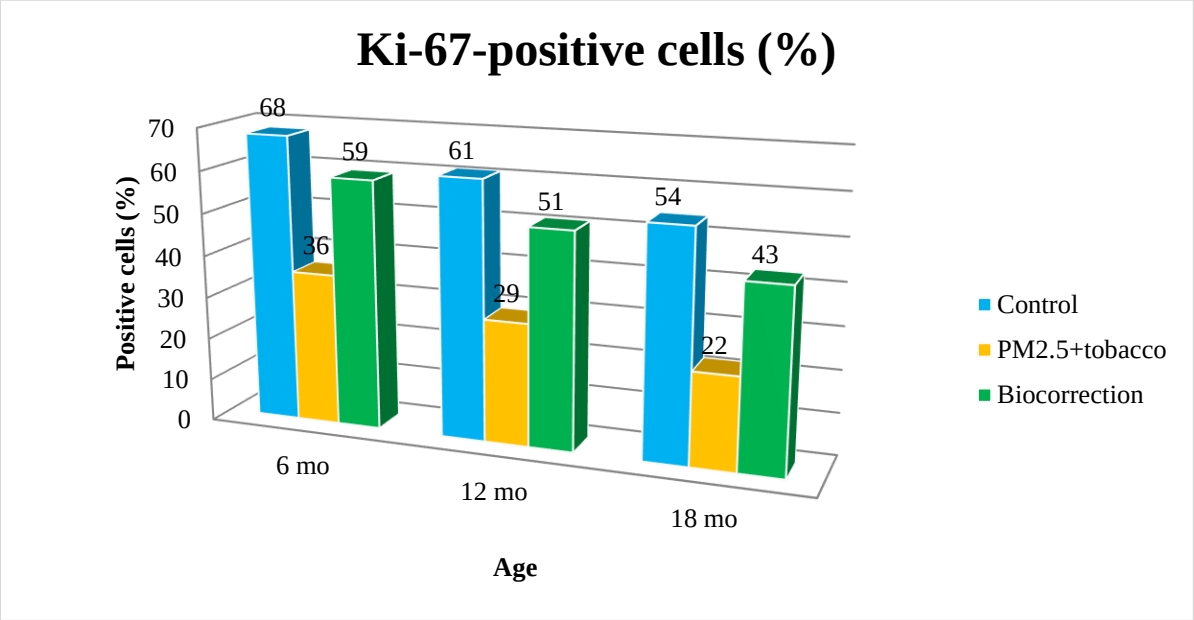

Diagram 1. Ki-67-positive cells (%) in the control, combined-exposure and biocorrection groups by age.

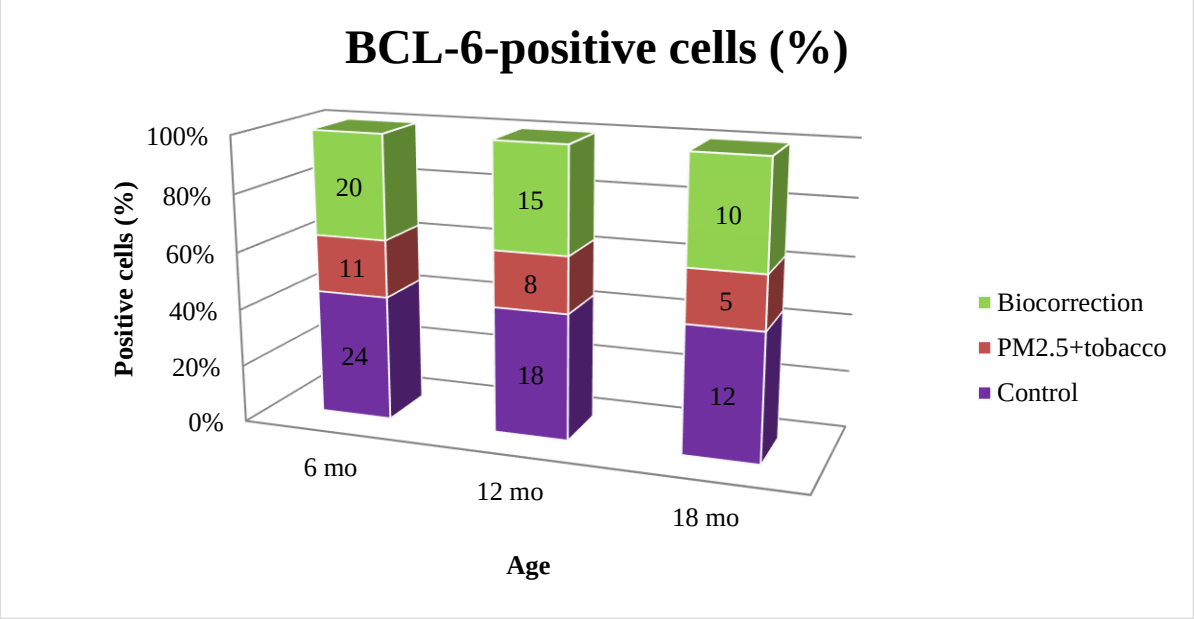

Diagram 2. BCL-6-positive cells (%) in the control, combined-exposure and biocorrection groups by age.

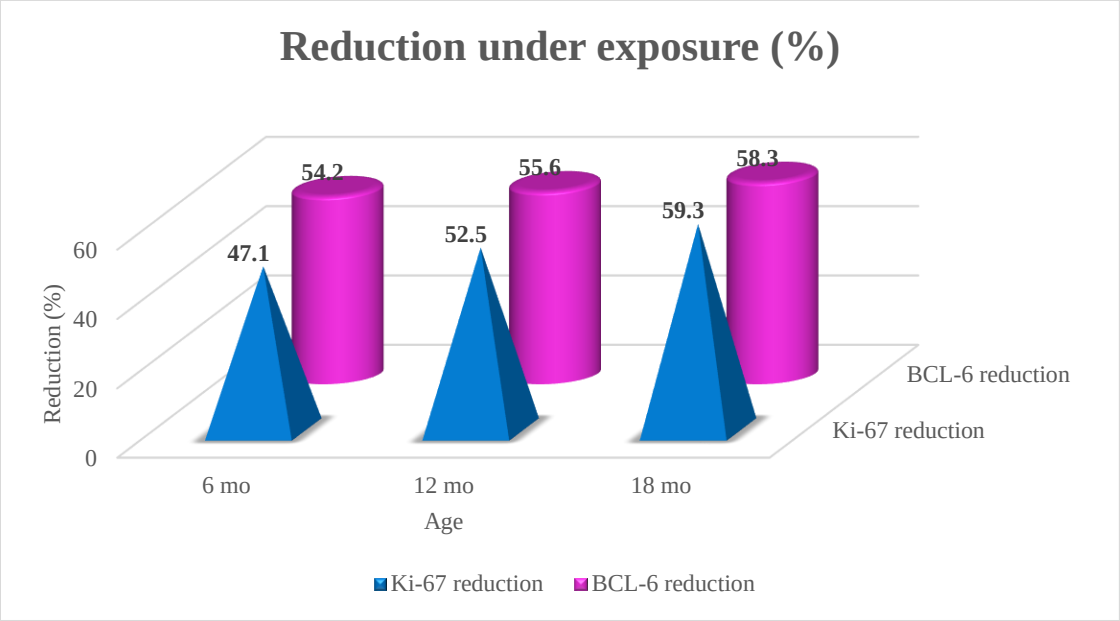

Diagram 7. Reduction of Ki-67 and BCL-6 under combined exposure relative to age-matched control (%).

3. Effect of biocorrection with Althaea officinalis

Biocorrection produced a clear positive shift of both markers toward control at every age. Ki-67-positive cells rose to 59% at 6 months (IRS 4→9), 51% at 12 months (IRS 4→9) and 43% at 18 months (IRS 2→4); BCL-6-positive cells rose to 20% (IRS 2→4), 15% (IRS 1→4) and 10% (IRS 1→2), respectively. Expressed as the proportion of the exposure-induced loss that was regained, the recovery rate for Ki-67 was 71.9%, 68.8% and 65.6% and for BCL-6 69.2%, 70.0% and 71.4% at 6, 12 and 18 months (Table 4, Diagrams 3, 4, 6). Notably, at 6 and 12 months the Ki-67 IRS returned fully to the control value (9), whereas at 18 months neither marker reached its control IRS, indicating an age-limited reparative reserve.

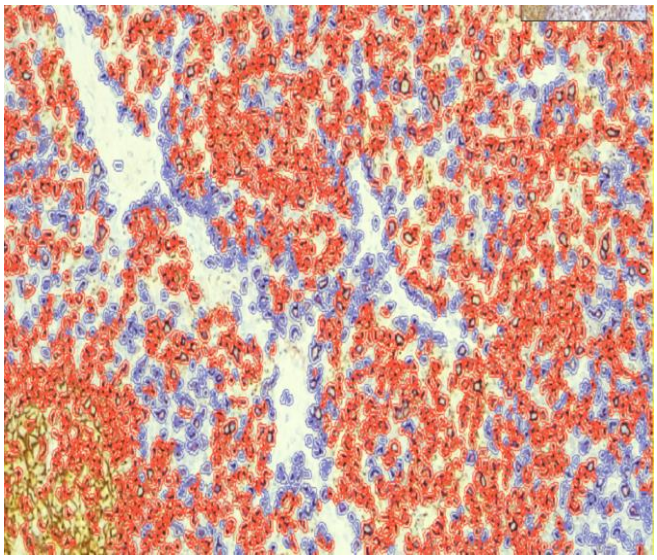

Figure 7. Micrograph placement — Ki-67, biocorrection group, 6-month rat. ×400, DAB. QuPath: 700 detected, 413 positive, 59% expression.

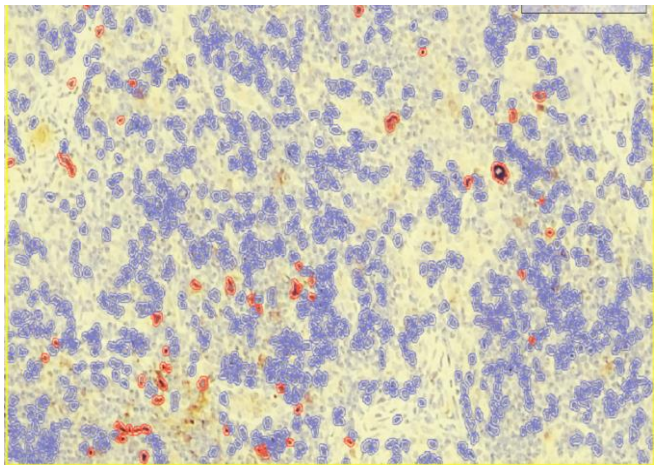

Figure 8. Micrograph placement — BCL-6, biocorrection group, 6-month rat. ×400, DAB. 20% expression.

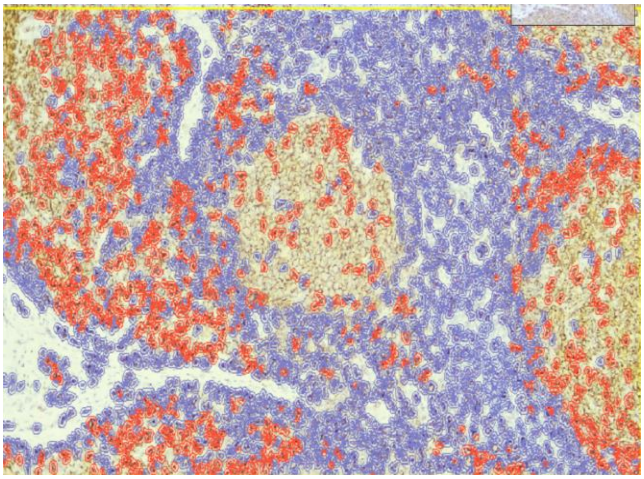

Figure 9. Micrograph placement — Ki-67, biocorrection group, 18-month rat. ×400, DAB. 43% expression; IRS 2→4 (incomplete normalization).

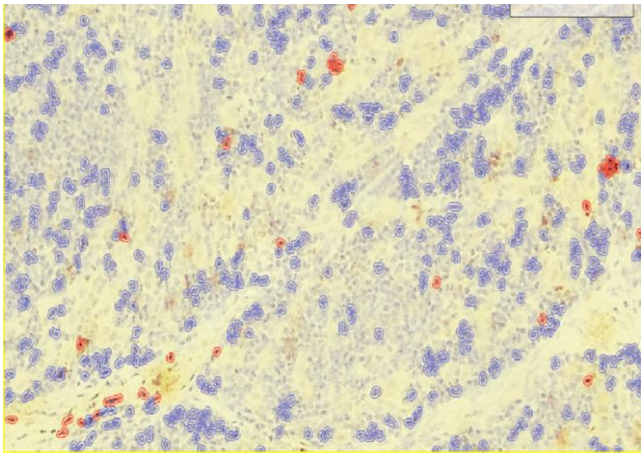

Figure 10. Micrograph placement — BCL-6, biocorrection group, 18-month rat. ×400, DAB. 10% expression.

Table 4. Comparative immunohistochemical efficacy of biocorrection

Age	Marker	Control, %	Exposure, %	Biocorr., %	Recovery, %	IRS (C/E/Bio)
6 mo	Ki-67	68	36	59	71.9	9 / 4 / 9
	BCL-6	24	11	20	69.2	6 / 2 / 4
12 mo	Ki-67	61	29	51	68.8	9 / 4 / 9
	BCL-6	18	8	15	70.0	4 / 1 / 4
18 mo	Ki-67	54	22	43	65.6	6 / 2 / 4
	BCL-6	12	5	10	71.4	4 / 1 / 2

Recovery rate = (biocorrection − exposure)/(control − exposure) × 100%.

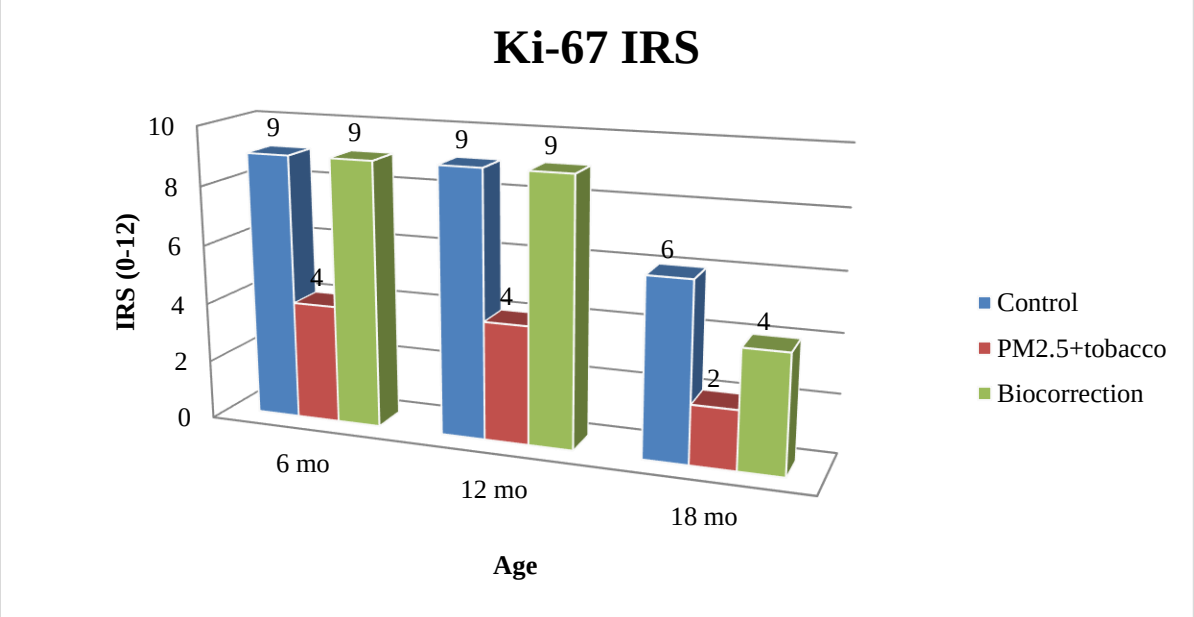

Diagram 3. Ki-67 IRS score in the control, combined-exposure and biocorrection groups by age.

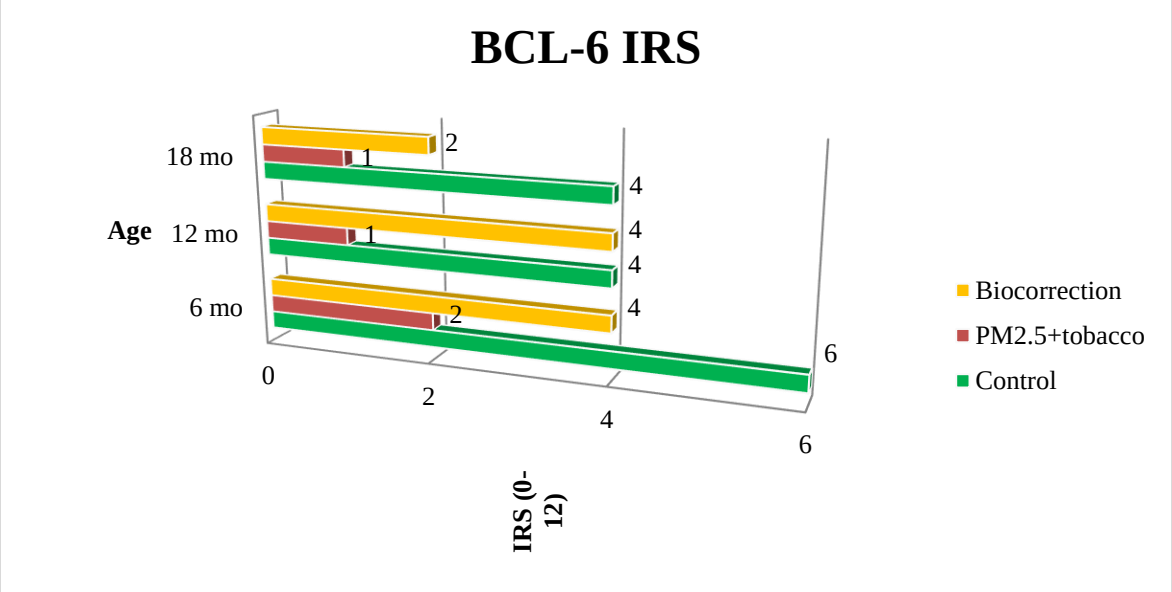

Diagram 4. BCL-6 IRS score in the control, combined-exposure and biocorrection groups by age.

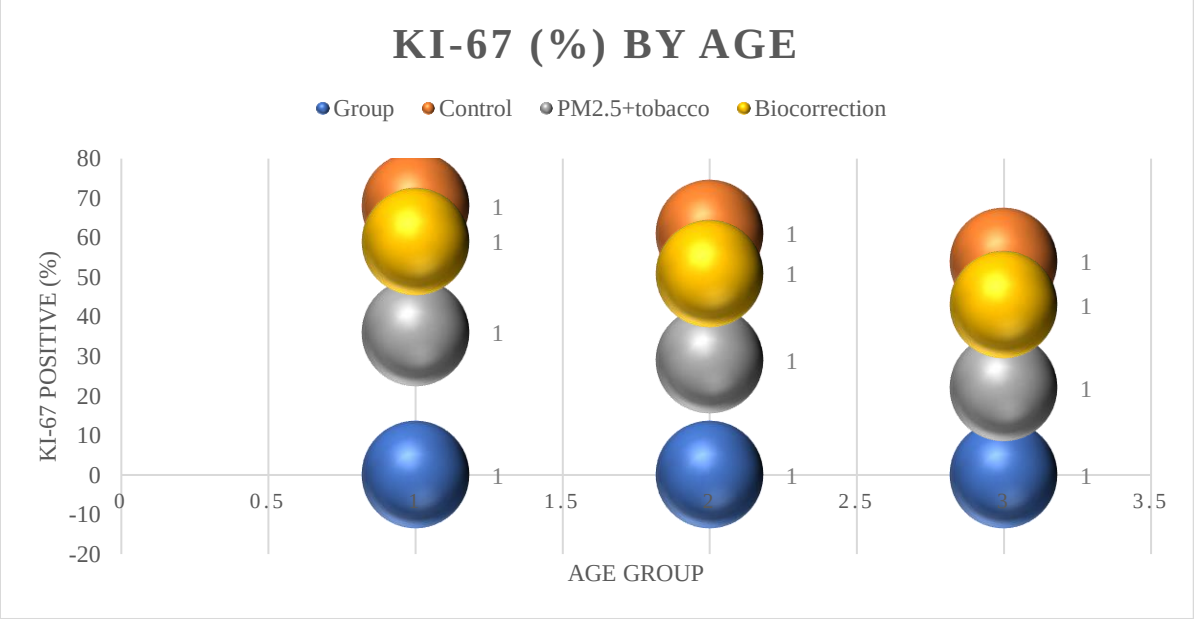

Diagram 5. Ki-67 (%) age dynamics across the three groups.

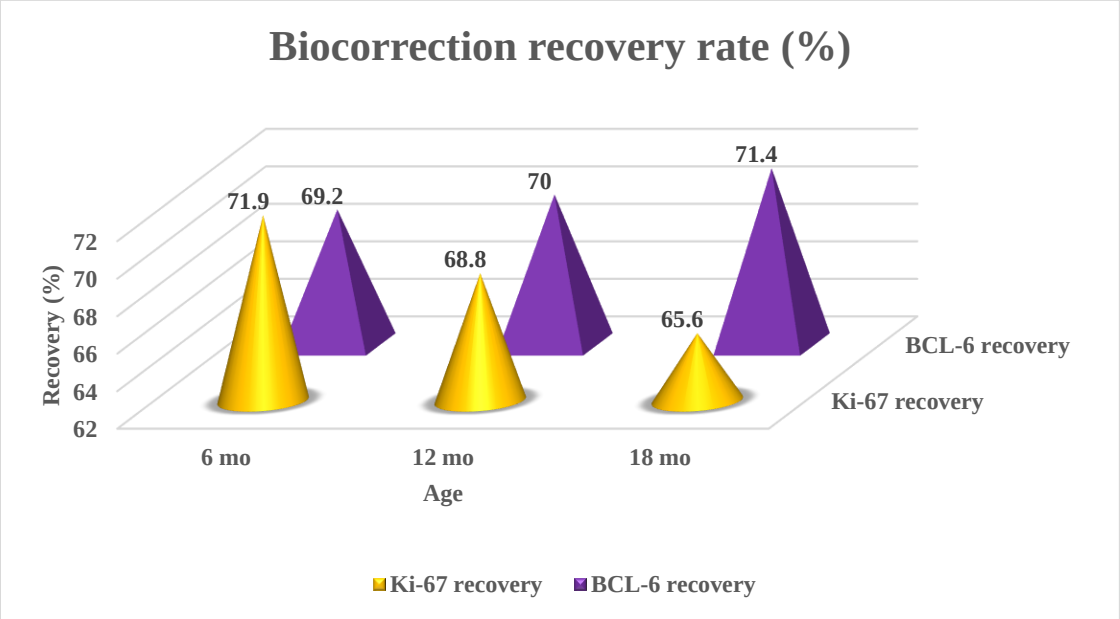

Diagram 6. Biocorrection recovery rate (%) for Ki-67 and BCL-6 by age.

Discussion

This study provides a quantitative, digitally analysed immunohistochemical account of how combined PM2.5 and tobacco-smoke inhalation reshapes the germinal-centre response of regional lymph nodes across the lifespan, and of its biocorrection. Three findings stand out: a physiological age-related decline of Ki-67 and BCL-6 in controls; a cumulative, age-aggravated "Ki-67↓ + BCL-6↓" suppression under combined exposure; and a marked but incomplete restoration after Althaea officinalis biocorrection.

The physiological decline of both markers in controls (Ki-67 68→54%, BCL-6 24→12%) is consistent with immunosenescence of the germinal-centre reaction and with evidence that lung-associated lymph nodes progressively accumulate inhaled particulates and lose immune competence with age [5; 6]. Interpreting the exposure effect therefore requires

comparison with the age-matched control rather than with absolute values — the approach adopted here through the reduction and recovery metrics.

Under combined exposure, the co-directional fall of Ki-67 and BCL-6 indicates that the injury is not confined to a single functional compartment but affects two coupled elements of the germinal-centre reaction: proliferative activity (Ki-67) and the BCL-6-defined B-cell program. This agrees with mechanistic reports that PM2.5 impairs adaptive immune responses and that chronic tobacco smoke and nicotine suppress T-cell help and attenuate antigen-specific germinal-centre and antibody (including IgA) responses in lung-associated lymphoid tissue [7; 8; 9; 10; 11]. The progressive deepening of the reduction with age (Ki-67 −47.1→−59.3%; BCL-6 −54.2→−58.3%) shows that the combined exposure does not merely reproduce the physiological age gradient but significantly amplifies it, so that the functional reserve of the germinal centre becomes increasingly limited in older animals. The parallelism between these immunohistochemical changes and the morphometric germinal-centre reduction strengthens the internal validity of the model, since two independent read-outs — structural morphometry and functional immunohistochemistry — point in the same direction.

Biocorrection with Althaea officinalis regained roughly two-thirds of the exposure-induced loss of both markers (recovery 65.6–71.9% for Ki-67 and 69.2–71.4% for BCL-6). This is biologically plausible given the documented antioxidant, anti-inflammatory and immunomodulatory properties of A. officinalis — attributable to its polysaccharides, flavonoids (kaempferol, quercetin) and phenolic acids — including protection of cells from reactive-oxygen-species-mediated injury and stimulation of phagocytosis [16; 17]. Importantly, the recovery was incomplete, particularly at 18 months, where neither marker reached its control IRS: the Ki-67 recovery rate declined slightly with age (71.9→65.6%), suggesting an age-limited proliferative reserve, whereas the BCL-6 recovery remained around 69–71% but over a progressively lower absolute expression (20→15→10%). The effect is therefore best interpreted not as absolute regeneration but as a pronounced protective and functionally restorative (immunomodulatory) action that shifts the damaged germinal-centre profile substantially back toward normal.

Strengths of the study include the use of two complementary markers, standardized digital (QuPath) quantification with paired cell counts, semiquantitative IRS scoring and an explicit recovery metric that controls for the physiological age gradient. Limitations are that the exposure parameters follow the experimental protocol and should be reported in full for reproducibility, that formal inferential statistics on larger per-group samples would further strengthen the descriptive comparisons, and that the micrographs indicated in Figures 1–10 correspond to the immunohistochemical illustrations of the dissertation and should be inserted at the marked positions.

Conclusion

1. In control rats, germinal-centre Ki-67 and BCL-6 expression declines physiologically with age (Ki-67 68→61→54%; BCL-6 24→18→12%) while zonal organization is preserved, defining a normal age-specific immunohistochemical profile.

2. Combined PM2.5 + tobacco-smoke exposure suppresses both markers at all ages and the effect intensifies with age: Ki-67 falls by 47.1%, 52.5% and 59.3% and BCL-6 by 54.2%, 55.6% and 58.3% relative to age-matched control, amplifying the physiological gradient.

3. The co-directional "Ki-67↓ + BCL-6↓" pattern, concordant with the morphometric germinal-centre reduction, indicates combined injury to both the proliferative and the BCL-6-defined B-cell components of the germinal-centre reaction.

4. Biocorrection with Althaea officinalis L. restores both markers toward control (recovery 71.9/68.8/65.6% for Ki-67 and 69.2/70.0/71.4% for BCL-6), with full IRS normalization of Ki-67 at 6 and 12 months but incomplete normalization at 18 months.

5. The biocorrective effect is best regarded as a protective and functionally restorative (immunomodulatory) action rather than absolute regeneration; Ki-67 and BCL-6 immunohistochemistry with IRS scoring provides sensitive criteria for detecting the exposure effect and for evaluating biocorrection efficacy.

References

1. Health Effects Institute. State of Global Air 2024. Special Report. Boston: HEI; 2024.
2. GBD 2021 Risk Factors Collaborators. Global burden and strength of evidence for 88 risk factors, 1990–2021. Lancet. 2024;403(10440):2162–2203.
3. World Health Organization. WHO global air quality guidelines. Geneva: WHO; 2021.
4. Jones IA, St. Helen G, Meyers MJ, et al. Biomarkers of secondhand smoke exposure in automobiles. Tob Control. 2014;23(1):51–57.

5. Ural BB, Caron DP, Dogra P, et al. Inhaled particulate accumulation with age impairs immune function and architecture in human lung lymph nodes. Nat Med. 2022;28(12):2622–2632.
6. Nikitin A. Effect of air pollution on the human immune system. Nat Med. 2022;28(12):2482–2483.
7. Zhao J, Li X, Chen Y, et al. Fine particulate matter manipulates immune response to exacerbate microbial pathogenesis in the respiratory tract. Eur Respir Rev. 2024;33(173):230259.
8. Miller GE, Passarelli V, Chen E, et al. Ambient PM2.5 and specific sources increase inflammatory cytokine responses to stimulators and reduce sensitivity to inhibitors. Environ Health Perspect. 2024;132(4):47009.
9. Sopori M. Effects of cigarette smoke on the immune system. Nat Rev Immunol. 2002;2(5):372–377.
10. Bhalla M, Nayerhoda R, Tchalla EYI, et al. Cigarette smoke exposure attenuates the induction of antigen-specific IgA in the murine upper respiratory tract. Mucosal Immunol. 2021;14(6):1359–1370.
11. Wang Q, Li X, Kobzik L, et al. Cigarette smoke modulates inflammation and immunity via ROS-regulated trained-immunity mechanisms. Antioxid Redox Signal. 2023;38(13):1041–1069.
12. Gerdes J, Lemke H, Baisch H, et al. Cell-cycle analysis of a cell-proliferation-associated human nuclear antigen defined by the monoclonal antibody Ki-67. J Immunol. 1984;133(4):1710–1715.
13. Hashmi AA, Iftikhar SN, Nargus G, et al. Ki-67 proliferation index in germinal and non-germinal subtypes of diffuse large B-cell lymphoma. Cureus. 2021;13(2):e13120.
14. Basso K, Dalla-Favera R. Roles of BCL6 in normal and transformed germinal center B cells. Immunol Rev. 2012;247(1):172–183.
15. Cheng Y, Xu K, et al. Correlation between C-MYC, BCL-2 and BCL-6 protein expression and gene translocation as biomarkers in DLBCL. Front Oncol. 2018;8:658.
16. Bonaterra GA, Bronischewski K, Hunold P, et al. Anti-inflammatory and anti-oxidative effects of Phytohustil® and root extract of Althaea officinalis L. on macrophages in vitro. Front Pharmacol. 2020;11:290.
17. Bonaterra GA, et al. Phytohustil® and root extract of Althaea officinalis L. exert anti-inflammatory and anti-oxidative properties and improve the migratory capacity of endothelial cells in vitro. Front Pharmacol. 2022;13:948248.
18. Remmele W, Stegner HE. Recommendation for uniform definition of an immunoreactive score (IRS) for immunohistochemical detection. Pathologe. 1987;8(3):138–140.
19. Bankhead P, Loughrey MB, Fernández JA, et al. QuPath: open source software for digital pathology image analysis. Sci Rep. 2017;7:16878.
20. Acs B, Pelekanou V, Bai Y, et al. Ki67 reproducibility using digital image analysis: an inter-platform and inter-operator study. Lab Invest. 2019;99(1):107–117.
21. Song JY, Kim H, et al. Comparison of Ki-67 labeling index patterns of DLBCL and Burkitt lymphomas using image analysis. Diagnostics. 2021;11(2):272.
22. Zhao Y, et al. An update on adverse health effects from exposure to PM2.5. Environ Adv. 2024;18:100603.
23. Snoderly HT, et al. Animal models and mechanisms of tobacco smoke-induced chronic obstructive pulmonary disease. J Toxicol Environ Health B. 2023;26(5):275–305.
24. Zhang N, Said A, Wischnewski S, et al. Semaphorin3E regulates germinal-centre responses in a mouse model of allergic airway inflammation. Front Immunol. 2021;12:634097.
25. Morissette MC, et al. Persistence of pulmonary tertiary lymphoid tissues and anti-nuclear antibodies following cessation of cigarette-smoke exposure. Respir Res. 2014;15:49.
26. Memarzia A, Khazdair MR, Behrouz S, et al. Anti-inflammatory, antioxidant and immunomodulatory effects of natural products relevant to lymphoid tissue protection. Phytother Res. 2021;35(6):2953–2977.